https://doi.org/10.5194/egusphere-2026-1198
Preprint. Discussion started: 4 May 2026

OhBemn (version 0.2): A Simple Boundary Element Method-model for Ocean Surface Waves

Gaute Hope[1], Patrik Bohlinger[1], Trygve Halsne[1], and Øyvind Breivik[1,2]

[1]Norwegian Meteorological Institute, Bergen, Norway.
[2]University of Bergen, Bergen, Norway.

Correspondence: Gaute Hope (gauteh@met.no / gaute.hope@gmail.com)

Abstract. A simple Boundary Element Method-model is implemented for ocean surface waves. The model is supplied with a framework for calculating source parameters, constructing boundaries, calculating sea surface elevation, and reflection coefficients at trenches or partially reflecting boundaries. The model is open source, and is based on the open source model for the acoustic Helmholtz equation developed in Kirkup (1998). It is implemented in Python and Rust, and may be installed as a regular Python-package.

This type of models are suitable for domains that are separated by a sharp boundary (constant wave speed in each domain), like abrupt depth transitions (submarine trenches), coastlines and harbours. It does not account for refraction in the domain, but is particular useful for calculating the interference patterns caused by reflection and diffraction. This offers a complementary strength to ray-tracing models, which are particularly useful for modeling refraction. The model is a simple tool for computationally cheap exploration of wave propagation, and for studying the underlying phenomena which are often difficult to separate in more advanced models.

We present the basic theory, and the boundary conditions for common situations like breakwaters and harbours, trenches (coupled with estimates of reflection coefficient), as well as partially and fully absorbing boundaries.

1 Introduction

Abrupt changes in bathymetry, coastlines, and harbours reflect and diffract surface waves. Understanding the causes of the resulting wave field often requires computationally costly simulations with numerical wave models. These models usually assume a particular input wave spectra, either with random phase, or assuming a particular phase-distribution. This requires that a new simulation are performed for each spectral distribution, and for the more advanced models a change in the input amplitude across the spectra also require a new simulation. Simpler models model phenomena separately, and are therefore sometimes useful to distinguish which mechanism is more important in shaping the resulting wave field. They require stronger assumptions on input spectra and wave propagation, but in return, the wave field may be calculated for different spectra and amplitude independently, so that generic transfer functions can be found. Secondly, they are generally far less computational intensive so that many difference scenarios can be explored quickly.

https://doi.org/10.5194/egusphere-2026-1198
Preprint. Discussion started: 4 May 2026

Ray tracing models, like those described in Halsne et al. (2023); Irving et al. (2025), are suitable for capturing refraction effects. However, they do not compute the phase resolved wave field directly. The Boundary Element Method (BEM), historically also known as the Boundary Integral Method, is a method that can be used to solve the wave field along the boundary of a domain given a source field and boundary conditions (Figure 1). It is suitable for computing the wave field due to reflection and diffraction, but does not account for refraction. It computes the phase resolved wave field, but the phase may be disregarded later. The wave-field is then computable at arbitrary points either in the interior, at the boundary, or in the exterior (Kirkup, 2019). The advantage of the ray tracing and BEM models is that they can quickly compute many different input directions and periods independently, so that for a different input spectra the computation can be re-used without performing a new solution.

The Boundary Element Method is therefore particularly useful for problems which can be separated into distinct domains, e.g. a break-water and the ocean, a coastline, or steep changes in the bathymetry. It is often used when analyzing structures and waves (e.g., Viswanathan et al., 2021; Belibassakis et al., 2020; 202, 2025; Zabala et al., 2021; Raghavan et al., 2024; Hall et al., 2022; Kurnia and Ducrozet, 2023; Liu; Hecht, 2026). The method is also suitable to model abrupt changes in the bathymetry, either in the vertical plane (e.g. Raichlen and Lee, 1978; Sgallari, 1983), or in the horizontal plane. In situations where it is not possible to define discrete domains with constant parameters, the method is sometimes combined with Finite Element Methods in the interior domain, or coupled with other methods. The difficulty in using the model is often to define the boundary-conditions and the incident wave-field at the boundary.

In this paper we build on the development in Kirkup (1998) made for acoustic waves in two-dimensions, and adapt the model to linear ocean waves. The resulting package is named *ohbemn* and is distributed openly[1]. Previous open-source implementations for acoustic waves in Fortran (Kirkup, 1998) and Python (Jargstorff, 2025) provided inspiration implementation. The model is adapted to ocean waves, and implemented in Python and Rust. The package is distributed as a Python-package (and Rust-package) which can be installed and used without any prior knowledge of Rust. The Python interface allows ease of use and accessibility, while Rust and parallel computation of matrix coefficients and solutions for sample points greatly speed up the model. Additionally, the solution for each wavenumber can be computed independently and in parallel. These may be summed either coherently or incoherently later to produce an amplitude transfer function or a response spectrum (Holthuijsen, 2007, Eq. 3.6.6.).

The implementation is open-source, with demonstration of various example situation. It is easily available to install and adapt. This makes the model a useful tool for understanding and BEM-modeling and investigating suitable problems.

2 Linear Ocean Waves and the Boundary Element Method

The linear wave equation is

$$\nabla^2\varphi - \frac{1}{c^2}\frac{\partial^2}{\partial t^2}\varphi = 0, \tag{1}$$

[1]https://github.com/gauteh/ohbemn

https://doi.org/10.5194/egusphere-2026-1198
Preprint. Discussion started: 4 May 2026

where $\nabla^2 = \sum \frac{\partial^2}{\partial x_i^2}$ is the Laplacian. Under assumption that the fluid under a wave undergoes irrotational motion (Holthuijsen, 2007, pp. 115–116), i.e., $\nabla \times \mathbf{u} = 0$, the velocity of the water particles can expressed through the *velocity potential*, φ, with components

$$\mathbf{u} = (u, v, w) = \nabla\varphi. \tag{2}$$

Here, u, v, and w are the water particle velocity components in the x and y, and z directions. Detailed derivations of the linear wave equation can be found in, e.g., Holthuijsen (2007); Kinsman (1965); Lamb (1932). The model described here is designed to simulate the field in the horizontal plane, at the surface.

With the additional assumption that the fluid is incompressible, we now have

$$\nabla \times \nabla\varphi = 0, \tag{3}$$

$$\nabla \cdot \nabla\varphi \equiv \nabla^2\varphi = 0. \tag{4}$$

Taking the Fourier transform of the wave equation (1), or separating φ on its temporal and spatial variables, results in the Helmholtz equation or the frequency-domain wave equation,

$$\nabla^2\varphi + k^2\varphi = 0. \tag{5}$$

Here, the separation constant $k^2 = \frac{\omega^2}{c^2}$ is the wave number. The Helmholtz equation is the wave equation in the frequency domain with a time dependence of $e^{i\omega t}$. The Helmholtz equation is solved for individual wave numbers and sources independently, which may be superimposed to find a full solution.

2.1 Kinematic and dynamic boundary condition

At the surface, the pressure is equal to the atmospheric pressure

$$\frac{\partial\varphi}{\partial t} + g\eta = 0\Big|_{z=0}, \tag{6}$$

Relating the surface to the velocity potential, and linearizing, yields

$$\frac{\partial\eta}{\partial t} = \frac{\partial\varphi}{\partial z}\Big|_{z=\eta}. \tag{7}$$

This is applied at the varying surface using a Taylor expansion and disregarding the quadratic terms,

$$\frac{\partial\eta}{\partial t} = \frac{\partial\varphi}{\partial z}\Big|_{z=0}. \tag{8}$$

Equation (8) is the surface kinematic boundary condition.

At the seabed the vertical velocity vanishes,

$$\frac{\partial\varphi}{\partial z} = 0\Big|_{z=-d}. \tag{9}$$

The surface elevation can be obtained from φ through differentiation of (6) in the frequency domain (multiplying by $i\omega$),

$$\eta = -\frac{i}{g} w\varphi. \tag{10}$$

https://doi.org/10.5194/egusphere-2026-1198
Preprint. Discussion started: 4 May 2026

2.2 The Boundary Element Method

The fundamental idea behind the Boundary Element Method is to reformulate the wave equation (Helmholtz equation) as an integral equation, rather than attempting to directly solve it. In this implementation the *direct* approach is used, based on *Green's second identity*,

$$\int_D \left[\varphi(\mathbf{q})\nabla^2\varphi(\mathbf{q}) - \psi(\mathbf{q})\nabla^2\psi(\mathbf{q})\right] dV_q = \oint_S \varphi(\mathbf{q})\frac{\partial\psi(\mathbf{q})}{\partial n_q} - \psi(\mathbf{q})\frac{\partial\varphi(\mathbf{q})}{\partial n_q} dS_q. \quad (11)$$

Using Green's third identity, on the inhomogeneous wave equation with a unit source, Green's function for the two-dimensional Helmholtz equation is then found (e.g. Sommerfeld, 1912),

$$[\nabla^2 + k^2]G_k(\mathbf{p},\mathbf{q}) = -\delta(\mathbf{p},\mathbf{q}). \quad (12)$$

This yields

$$G_k(\mathbf{p},\mathbf{q}) = \frac{i}{4}H_0^{(1)}(kr). \quad (13)$$

Where $r = |\mathbf{p}-\mathbf{q}|$. Solving the Helmholtz equation (5) for $\nabla^2\varphi$ and substituting into (11), and setting $\psi = G_k$, the boundary integral equation is obtained (by virtue of the Dirac delta function),

$$\int_S \frac{\partial G}{\partial n_q}(\mathbf{p},\mathbf{q})\varphi(\mathbf{q})dS_q - \int_S G(\mathbf{p},\mathbf{q})\frac{\partial\varphi}{\partial n_q}dS_q = -\frac{1}{2}\varphi(q) \in \partial S. \quad (14)$$

The full definition of (14) for both the interior and the exterior is derived in detail in Kirkup (1998) and in Kirkup (2019, Eqs. 14 and 30). As mentioned, this implementation follows the development for acoustic waves in Kirkup (1998), but here adapted to ocean waves.

The method formally describes Huygens' principle where Green's function acts as a unit source along the boundary, and the wave field may be determined from integrating the contribution from all the unit sources. The integral equation, (14), relates the potential (and its derivative) only at the boundary and once it is solved the field is computable at any point in the interior or exterior.

2.2.1 Discretization

To solve the boundary integral equation (14) and compute the wave field at the boundary, the continuous boundary between the interior and exterior (Fig. 1) must be discretized (expecting the segments to defined in the clockwise direction). In this implementation a single simply connected boundary is allowed, but discontinuities and more complicated domains are generally

https://doi.org/10.5194/egusphere-2026-1198
Preprint. Discussion started: 4 May 2026

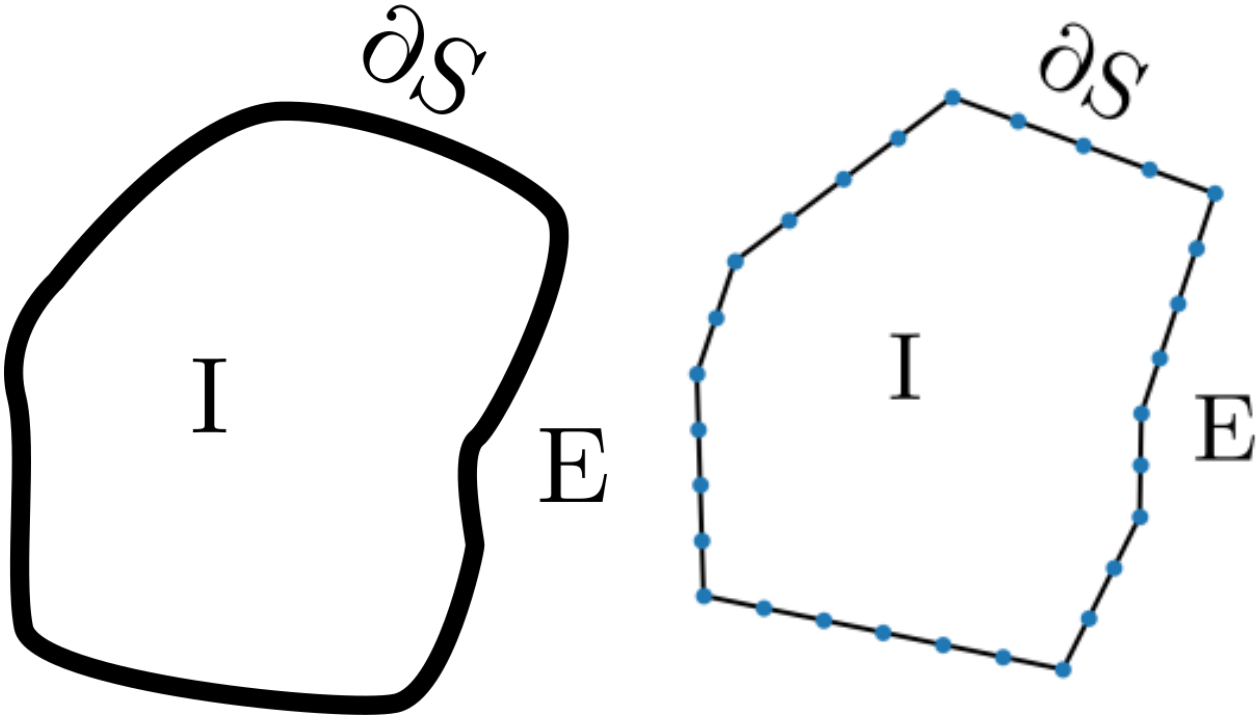

Figure 1. The domain in the Boundary Element Method: Interior (I), exterior (E), and boundary ∂S. The continuous domain (left) must be discretized into segments (right).

possible, Kirkup 1997) There are several ways of doing this, but here we use a simple method of linear segments. The wave field is constant at each segment (*colocation*), requiring the number of segments to be sufficiently high. The contribution to the wave field along one segment is summed using numerical quadrature (Gauss-Legendre).

The integral equation can now be written as linear operators working on the velocity potential or its derivatives. Depending on which is known, the other can be solved as a set of linear equations for each boundary segment. The potential and its derivative can then be found as a matrix multiplication for any point in the interior or exterior domain.

2.3 Boundary conditions

Typically, either the velocity potential φ, or the normal derivative across the boundary $\frac{\partial \varphi}{\partial n}$ must be known at the boundary (*Dirichlet* or *Neumann* boundary conditions, respectively). This can be determined either from a source inside the domain, where the boundary acts as a source in the external and a reflecting boundary in the interior, or from a source outside the domain, where the boundary acts as a scatterer in the exterior or a source in the interior.

Either the Dirichlet or the Neumann condition specify the wave field at the boundary, so both cannot be specified independently at the same time. A boundary condition specified as a linear combination of the two is called the *Robin* boundary

https://doi.org/10.5194/egusphere-2026-1198
Preprint. Discussion started: 4 May 2026

condition and may be applicable in some situations (e.g., Eq. (16)), or as as an approximation in certain situations,

$$\alpha\varphi + \beta\frac{\partial\varphi}{\partial n} = f. \tag{15}$$

The boundary conditions are specified through the constants α, β and f in Eq. (15) at each segment. Additionally, an incident field may be specified for φ and $\frac{\partial\varphi}{\partial n}$.

This model is developed for modeling the surface waves in the horizontal plane (i.e., the wave number cannot change within each domain). The surface and bottom boundary conditions determine the wave speed, as well as the relation between the velocity potential and the sea-surface elevation (η) and the particle velocities.

2.3.1 Sommerfeld radiation condition

The Sommerfeld radiation conditions says that there are no incoming waves, only outward radiating waves from a point or a boundary. In the exterior the fundamental solution (Green's function) already implements the Sommerfeld condition. Solving for the interior, I, at the boundary the Sommerfeld radiation condition, *an absorbing boundary*, is specified as a relation between the potential and the normal derivative (Sommerfeld, 1912, p. 334),

$$\frac{\partial\varphi}{\partial n} = -ik\varphi. \tag{16}$$

The normal derivative (note that the spatial derivative is equivalent to a multiplication in the wave number domain: $\frac{\partial}{\partial x} = ik_x$) is pointing outwards, so that the sign before i is inverted for an exterior problem. This is a *Robin* boundary condition.

2.3.2 Partially reflecting or transmitting boundary

A partially reflecting boundary may occur either between abrupt depth changes, or at partially reflecting beaches, or at partially absorbing structures like breakwaters. If the reflected or transmitted wave field (either φ or $\frac{\partial\varphi}{\partial n}$) is already known through other means at the boundary, it can be assigned along the segments, and the resulting wave field may be computed elsewhere. To calculate the reflected or transmitted wave it is customary to simplify the problem to a plane wave encountering an interface.

For a continuous fluid the surface must be continuous, and the particle velocity across the boundary must thus also be continuous

$$\varphi_1 = \varphi_2 \quad \text{and} \quad \frac{\partial\varphi_1}{\partial n} = \frac{\partial\varphi_2}{\partial n} \quad \text{at } \partial S. \tag{17}$$

The incident and reflected wave must be equal to the transmitted wave at the interface,

$$\varphi_i + \varphi_r = \varphi_t \qquad \text{at } \partial S \tag{18}$$

$$\frac{\partial\varphi_i}{\partial n} + \frac{\partial\varphi_r}{\partial n} = \frac{\partial\varphi_t}{\partial n} \qquad \text{at } \partial S. \tag{19}$$

With the amplitudes ($a_{i,r,t}$) of the waves, $\varphi_{i,r,t} = a_{i,r,t}\exp(i\omega t - ikx + \theta_{i,r,t})$, the reflection and transmission coefficients are defined as the ratios:

https://doi.org/10.5194/egusphere-2026-1198
Preprint. Discussion started: 4 May 2026

$$T = \frac{a_t}{a_i}, \quad R = \frac{a_r}{a_i} \tag{20}$$

The wave energy is approximately proportional to the square of the amplitude ($E = \frac{1}{2}\rho g a^2$, sum of potential and kinetic energy) (Holthuijsen, 2007). Between transmitted and reflected waves the energy is conserved:

$$|T|^2 + |R|^2 \equiv 1 \tag{21}$$

However, requiring both the sea-surface to be continuous (17) and the energy to be conserved (21) is not necessarily possible for partial reflections in this model, except at total reflection or total transmission. Other models are therefore usually necessary to capture the phenomena more properly for partially-reflecting boundaries in the ocean (e.g. Kirby and Dalrymple, 1983; Li et al., 2021). When the amplitude of the reflected or transmitted wave is unknown, the boundary condition of a partially reflecting boundary may be approximated as a mixed boundary condition (Robin). Berkhoff (1976) describes a method for this using complex reflection coefficients dependent on incidence angle and phase-shift:

$$\frac{\partial \varphi}{\partial n} + \alpha k \varphi = 0 \tag{22}$$

In this case, $\alpha = (\alpha_1 + i\alpha_2)$ is a complex transmission coefficient. The complex transmission coefficient may be calculated from the desired reflection coefficient (R), phase shift (β) and incidence angle (γ). This is easily computed for an incident field of either a point source or plane waves, but in the computed domain this is not known in advance. However, Isaacson and Qu (1990) found that the resulting field appears to be not very sensitive to the incidence angle (γ), and also suggest that the angle may be calculated from the direction of the wave field,

$$\theta = \arctan\left(\frac{\partial\varphi/\partial y}{\partial\varphi/\partial x}\right), \tag{23}$$

so that the incidence angle along the boundary can be calculated iteratively through $\gamma = \pi - \chi + \theta$ (here, χ is the angle between the segment normal and the x-axis, γ is for example initially set to 0). In the BEM, the normal velocities are already calculated at the boundary, so that it should be possible to obtain the wave direction directly from the solution.

The coefficients α_1 and α_2 are computed as

$$\alpha_1 = \frac{2R\sin\beta\cos\gamma}{1+R^2+2R\cos\beta} \tag{24}$$

$$\alpha_2 = \frac{(1-R^2)\cos\gamma}{1+R^2+2R\cos\beta}. \tag{25}$$

A perfectly reflecting boundary ($R = 1$) results in $\alpha = 0$ (Neumann boundary condition, hard boundary), while no reflection ($R = 0$, fully absorbing) corresponds to $\alpha = i$, a Sommerfeld radiation condition (16).

https://doi.org/10.5194/egusphere-2026-1198
Preprint. Discussion started: 4 May 2026

2.4 Plane-wave source

A plane wave is expressed by

$$\varphi = \hat{\varphi} \exp i(k_x x + k_y y). \tag{26}$$

The normal derivative of the source, $\frac{\partial \varphi}{\partial n}$, is often required. The directional derivative of a function f in the direction of the unit vector $\mathbf{n}$ is found through the *gradient* and the directional vector,

$$\frac{\partial f}{\partial n} \equiv \nabla_{\mathbf{n}} f = \nabla f(\mathbf{x}) \cdot \mathbf{n}, \tag{27}$$

For a plane wave, the gradient is given as

$$\frac{\partial \varphi}{\partial n} \equiv \nabla_{\mathbf{n}} \varphi = \hat{\varphi} \begin{bmatrix} -ik_x \\ -ik_y \end{bmatrix} \exp\left[i(k_x x + k_y y)\right]. \tag{28}$$

The plane-wave (1D) solution is the basis for finding the *dispersion relation* (e.g. Lamb, 1932; Kinsman, 1965; Holthuijsen, 2007),

$$\omega^2 = gk \tanh(kd) \tag{29}$$

with phase speed

$$c = \frac{dx}{dt} = \frac{\omega}{k}. \tag{30}$$

Further, the depth-dependent (evanescent) amplitude of the velocity potential, given a plane wave with surface amplitude a, becomes

$$\hat{\varphi} = \frac{\omega a}{k} \frac{\cosh[k(d+z)]}{\sinh(kd)}. \tag{31}$$

This leads to zero vertical particle velocity at the sea floor ($z = -d$) in accordance with the kinematic boundary condition at the bottom (Eq. (9)).

2.5 Attenuation of Swell

Attenuation or other reduction of the amplitude of the waves due to dissipation, or due to incoherence over time, can be implemented by assigning a complex wavenumber. The complex wavenumber defines the attenuation per meter.

Examples of empirical estimates of the dissipation of swell over long distances is given by Ardhuin et al. (2009); Collard et al. (2009); Jiang et al. (2016). The dissipation varies, but is of the order of

$$\mu = 3.7 \times 10^{-7} \qquad [\mathrm{m}^{-1}] \tag{32}$$

for the significant wave height.

https://doi.org/10.5194/egusphere-2026-1198
Preprint. Discussion started: 4 May 2026

For plane waves, the wave number with attenuation is (sign in front of imaginary part is dependent on sign of spatial wave, Jensen et al. 2011),

$$k = k' + ik''. \tag{33}$$

In this implementation, the boundary emits Green's functions based on the Hankel function (Eq. (13)), not plane waves. However, for large arguments, the Hankel function (H) has an asymptotic approximation,

$$H_0^{(1)}(kr) \sim \sqrt{\frac{2}{\pi kr}} \exp\left[i\left(kr - \frac{\pi}{4}\right)\right]. \tag{34}$$

Inserting the modified wave number with attenuation into (34) gives a small contribution from the leading $\frac{1}{\sqrt{k}}$ term, with an attenuation of $e^{-k''r}$ from the exponential factor. These contributions have *almost* the same effect as the plane-wave attenuation coefficient (Fig. 2), and the error is assumed to be within the margin of error of the empirically estimated attenuation coefficients. The units of k'' are *nepers per meter* [Np/m],

$$k'' = \ln\left(\frac{A_0}{A_x}\right)/x = \ln\left(\frac{1}{1-\sqrt{\mu}}\right)/1. \tag{35}$$

Here $\sqrt{\mu}$ implies that the amplitude is proportional to the square root of the significant wave height (Holthuijsen, 2007, Chap. 3.5). The attenuation can now be approximated as

$$k'' \approx \sqrt{\mu} + \mathcal{O}(\mu) \qquad \text{for small } \mu. \tag{36}$$

https://doi.org/10.5194/egusphere-2026-1198
Preprint. Discussion started: 4 May 2026

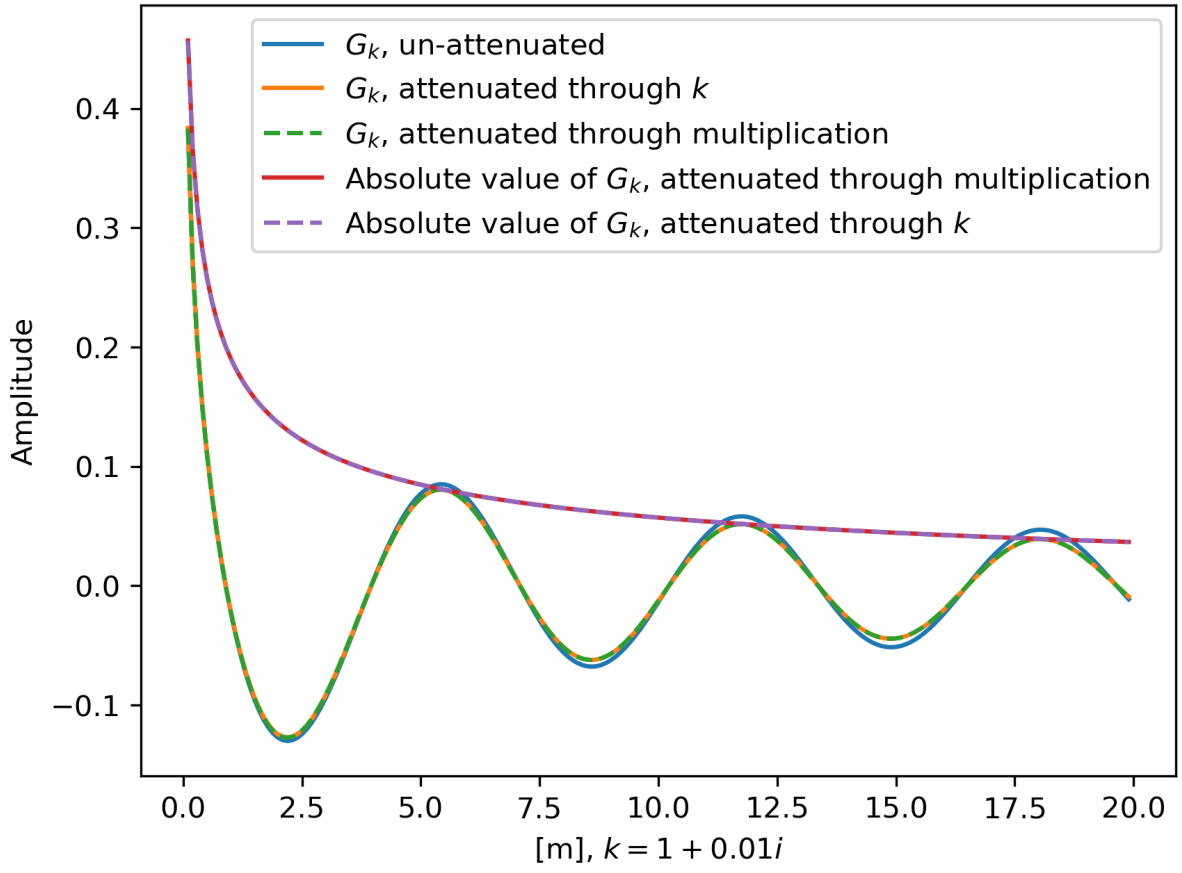

Figure 2. Attenuation for G_k and its asymptotic approximations, showing that a complex wave number approximates the plane-wave attenuation.

3 Implementation, structure, usage, and tests

This implementation is based on the derivation in Kirkup (1998) of a BEM model for acoustic waves. The Fortran code there and the Python code presented by Jargstorff (2025) served as inspiration for this project. The method has been adapted to ocean waves, including routines to aid in setting up the domain and some of the boundary conditions which may occur in the ocean. It has been re-implemented in a *Rust* core, but with a Python interface, so that it may be invoked as a regular Python package. The computational core has been parallelized of several of the computational steps.

The package may either be compiled from source or the python package index (PyPI), or installed from pre-compiled conda packages.

https://doi.org/10.5194/egusphere-2026-1198
Preprint. Discussion started: 4 May 2026

3.1 Usage

Listing 1 shows the basic set up of the model, consisting of: (1) calculating the parameters of the source, (2) defining the region, (3) defining the boundary conditions along each segment of the boundary, (4) solving the wave field at the boundary satisfying the boundary conditions, (5) using the boundary solution to calculating the wave field at arbitrary points.

Listing 1. Setting up and running the model.

```
import numpy as np
import ohbemn as oh

# Source, phase-speed and wavenumber (1)
c, cg, k = oh.wave.wavec_interm(T=8., h=40.)
kx = k / 2  # 45 deg. oblique direction.
ky = np.sqrt(k**2 - kx**2)

# Region (using example rectangle) (2)
region = oh.Region.rectangle(200, 200, 32, 32)

# Boundary conditions (3)
bc = region.boundary_condition()

centers = region.centers()
normals = region.normals()
bi = region.boundary_incidence()

for i, (x, n) in enumerate(zip(centers, normals)):
    # A plane source with phase = 0 at x, y = (0, 0)
    phi = oh.source.plane(kx, ky, *x)[0]
    # or: v = source.dplane(kx, ky, *x, -n)[0]

    bc.alpha[i] = 1.  # Dirichlet BC
    bc.beta[i] = 0.
    bc.f[i] = phi

# Solve the boundary oriented towards the interior (4)
solver = oh.Solver(region)
boundary_solution = solver.solve_boundary(oh.Interior,
                                          k, c, bc, bi)

# Solve field at 20x20 points in the interior (5)
xx, yy = np.meshgrid(np.linspace(0.01, 200, 10),
                     np.linspace(0.01, 200, 10))
p = np.vstack((xx.ravel(), yy.ravel())).T

Fp = boundary_solution.solve_samples(np.zeros(p.shape[0]), p)
```

https://doi.org/10.5194/egusphere-2026-1198
Preprint. Discussion started: 4 May 2026

3.2 Tests

Both the *Rust* and *Python* libraries are tested using unit tests and integration tests. The quadrature functions, integrator operators, and solver is tested on known problems and must match within numerical accuracy.

4 Applications of the BEM model

In the following sections several cases are shown which demonstrate the approximations and uncertainties of the method, and which simulation problems it may be useful for.

4.1 Water-water

Theoretically, both the surface elevation and the velocity across the boundary must be continuous (see Sec. 2.3.2). Since they are related, only one is specified at the time in this case (thus not necessarily conserving energy, which is not really possible to satisfy without more degrees of freedom). Listing 2 shows how the boundary conditions are defined when the amplitude of the transmitted and reflected wave is known.

Listing 2. Boundary condition specification for interior and exterior wave.

```
# Interior (transmitted)
At          = 0.6
bc.alpha[i] = 1
bc.beta[i]  = 0
bc.f[i]     = At * phi

# Exterior (reflected)
Ar          = 0.4
bc.alpha[i] = 1
bc.beta[i]  = 0
bc.f[i]     = -Ar * phi
```

Figure 3 shows the amplitude of a plane wave reflected and transmitted at a boundary for either total transmission or partial transmission. The sum of the incident and reflected wave is equal to the transmitted wave, so that the total surface ($\propto \varphi$) is always continuous.

In Figure 4 a rectangular interior with the exact same phase speed (and wave number) as the exterior is shown ($d = 40$ m, $T = 8$ seconds). A source emits plane waves obliquely incident on to the rectangular interior (Eq. (26)). The field as calculated without an interior domain is shown in the first column, secondly the interior domain calculated using the BEM from the boundary for the interior is shown, the final column shows both solutions overlaid. The methods yield identical results, and the field appears continuous.

The first row of panels shows the field calculated using the Dirichlet boundary conditions at the boundary, while the second uses the Neumann boundary conditions (specifying $\frac{\partial \varphi}{\partial n}$).

https://doi.org/10.5194/egusphere-2026-1198
Preprint. Discussion started: 4 May 2026

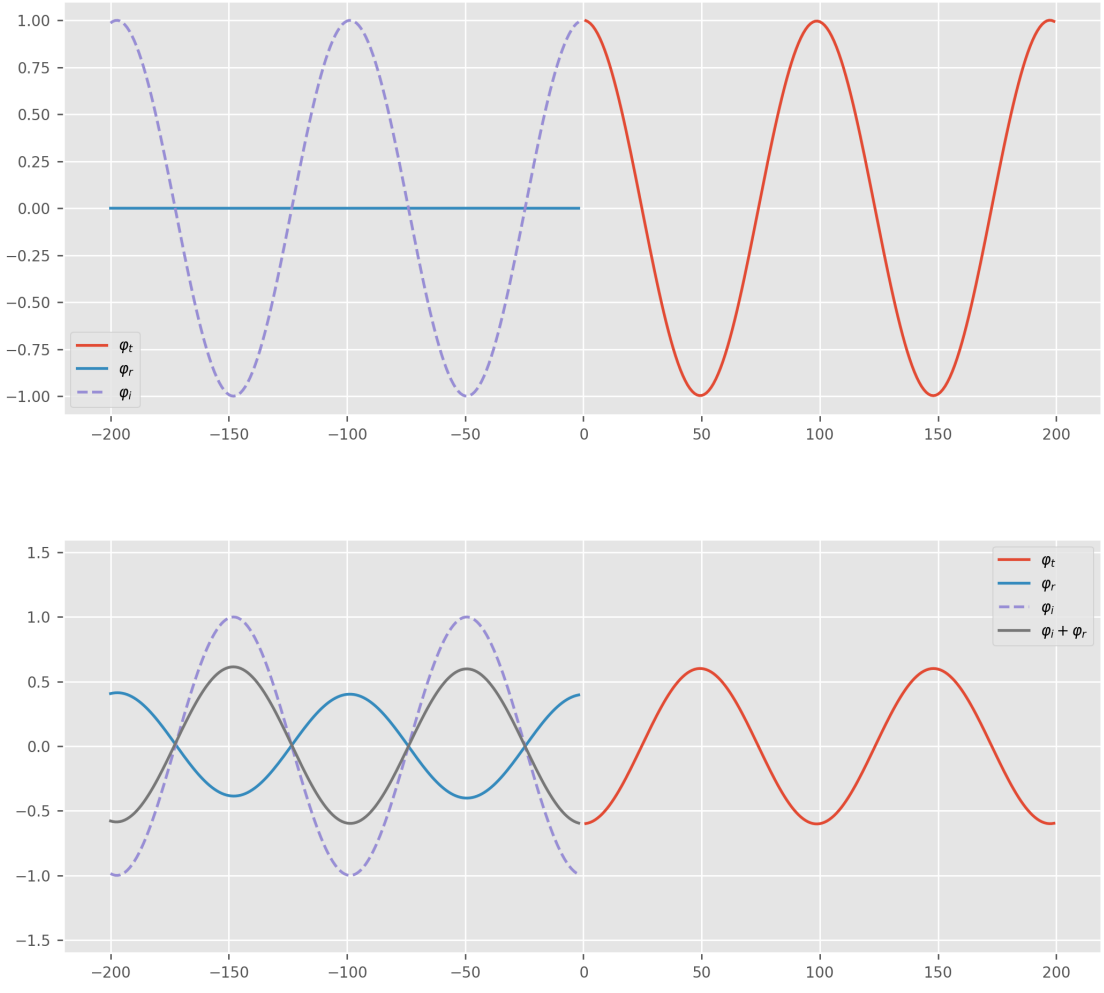

Figure 3. Fluid-fluid transmitted and reflected wave, total transmission (upper), partial transmission (lower).

https://doi.org/10.5194/egusphere-2026-1198
Preprint. Discussion started: 4 May 2026

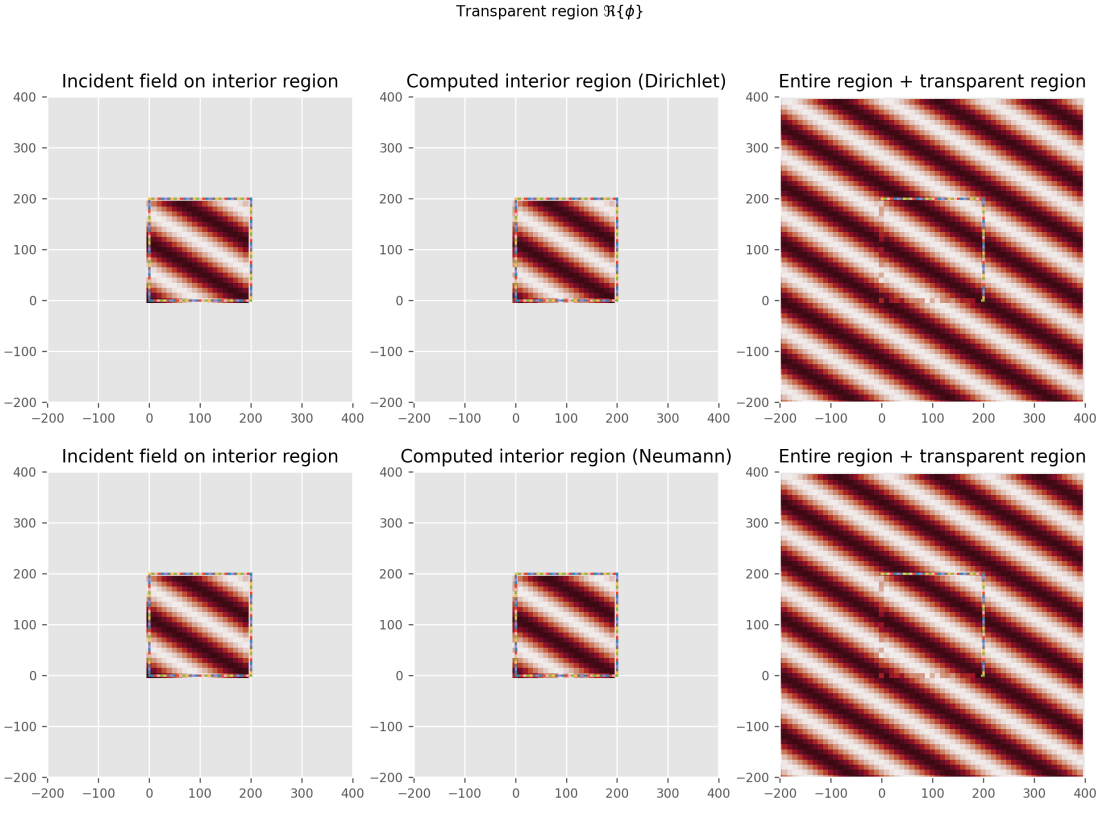

Figure 4. Transparent region, defined with either Dirichlet or Neumann boundary conditions.

https://doi.org/10.5194/egusphere-2026-1198
Preprint. Discussion started: 4 May 2026

4.2 Water-solid structure: Breakwater)

Waves encountering solid rock are free to move in the vertical direction (free surface), while the velocity at the boundary must become zero (e.g. Penney and Price, 1952; Chakrabarti and Sahoo, 1997; Pos and Kilner, 1987).

$$\frac{\partial \varphi}{\partial n} = 0 \Big|_{x \in \partial S}, \tag{37}$$

which is specified as a *Neumann boundary condition*. The boundary in the interior is non-reflecting and is set to the radiation boundary condition (16).

A harbor with a single opening, analogous to the *single slit* experiment is shown in Figure 5. The opening is located at the center of the bottom of the rectangular harbor. The opening is defined using Dirichlet boundary conditions with φ set by the incoming plane wave. Elsewhere on the sea-ward facing side, the boundary is set to a hard reflecting boundary, $\frac{\partial \varphi}{\partial n} = 0$. Inside, along the sides and at the far end of the harbor the boundary is set to be absorbing (simulating, e.g., a rocky beach which will dissipate rather than reflect the waves) using the Sommerfeld radiation condition, Eq. (16).

https://doi.org/10.5194/egusphere-2026-1198
Preprint. Discussion started: 4 May 2026

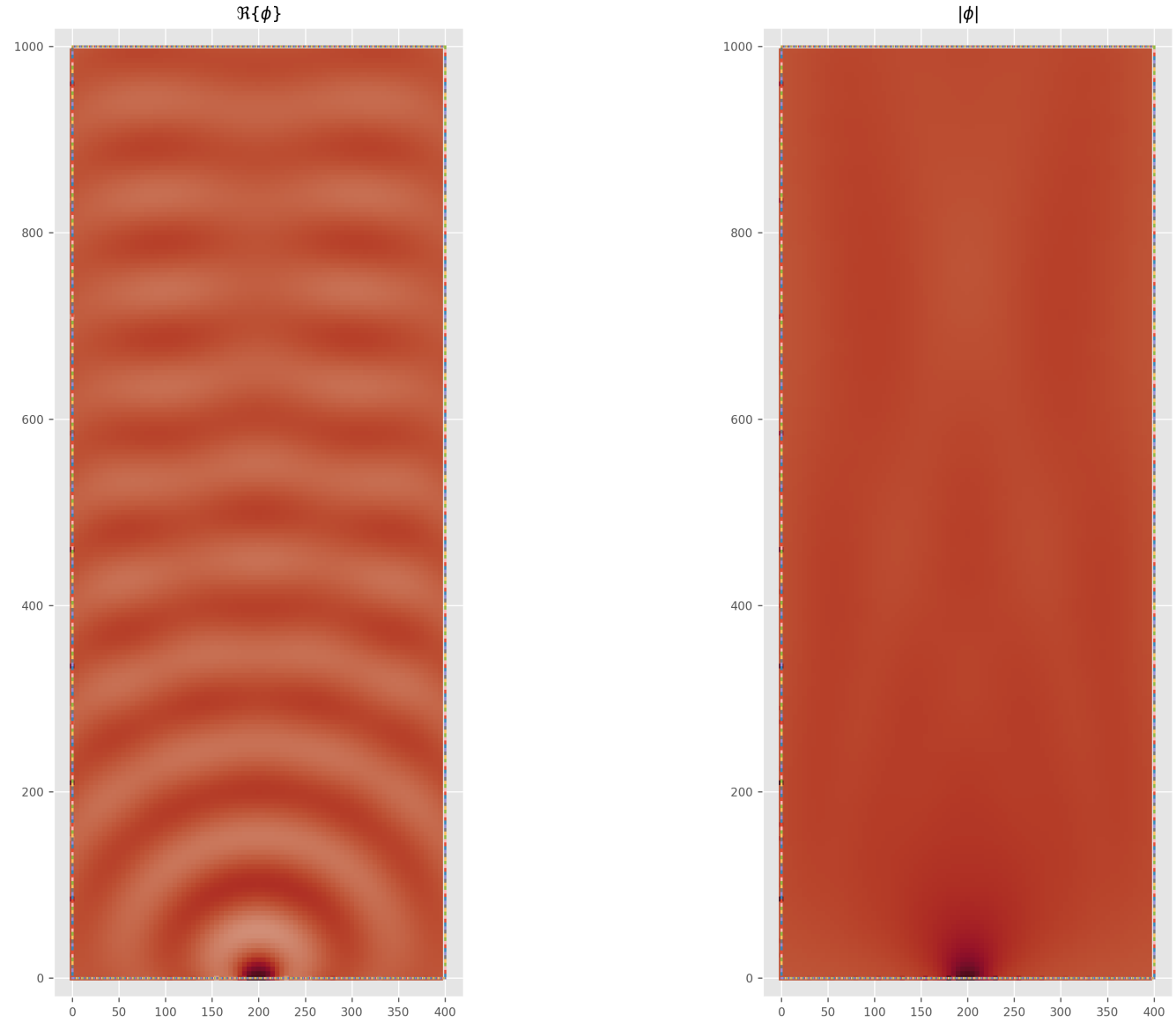

Figure 5. Breakwater (single slit), left: real part of φ at $t = 0$. Right: $|\varphi|$.

In Figure 6 the diffraction is calculated using the Rayleigh-Sommerfeld integral through the Fast Fourier Transform (FFT) (Shen and Wang, 2006) using the *diffractio* package (Sanchez-Brea et al., 2024). An opening of 24 meters is placed with the center at $x = 0$. The source is a plane wave with wavelength $\lambda \simeq 6.234$ meters. The diffracted amplitude along the x-axis is shown for $y = 100$ meters.

https://doi.org/10.5194/egusphere-2026-1198
Preprint. Discussion started: 4 May 2026

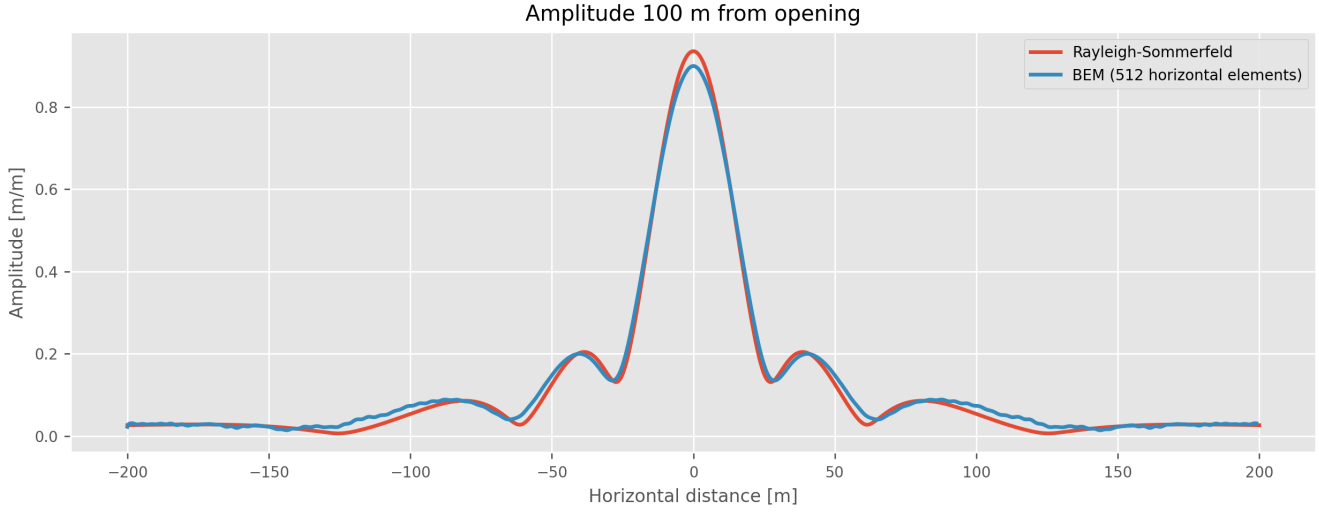

Figure 6. Comparison of diffracted amplitude at 100 m distance from the opening with diffraction computed using the Rayleigh-Sommerfeld integral (Shen and Wang, 2006; Sanchez-Brea et al., 2024).

Listing 3 shows how to define the boundary condition for a breakwater, with an opening, in this BEM model. Figures 5 and 6 use a radiating boundary (except at the opening), while Figure 7 uses Berkhoff (1976)'s method, Eq. (22), with a partially reflecting interior ($R = 0.7$).

Listing 3. Definition of boundary conditions for a breakwater, with an opening, for configurable reflection in the interior.

```
import ohbemn as oh

## Reflection coefficient
R = .7
alpha = oh.rcoeff.berkoff_partial_reflection(R)

## Boundary conditions
for i in range(region.len()):
    x = centers[i, :]
    n = normals[i, :]

    # Incident field
    phi = source.plane(0, k, *x)
    v = source.dplane(0, k, *x, -n)

    # opening
    if x[1] < 0.1 and (x[0] >= x0 and x[0] <= x1):
        bc.alpha[i] = 1.
        bc.beta[i] = 0.
        bc.f[i] = phi
    else:
```

https://doi.org/10.5194/egusphere-2026-1198
Preprint. Discussion started: 4 May 2026

```
# Radiating / absorbing boundary
# bc.alpha[i] = 1j * k
# bc.beta[i] = 1.
# bc.f[i] = 0

# Partially reflecting boundary
bc.alpha[i] = alpha * k
bc.beta[i] = 1.
bc.f[i] = 0.
```

https://doi.org/10.5194/egusphere-2026-1198
Preprint. Discussion started: 4 May 2026

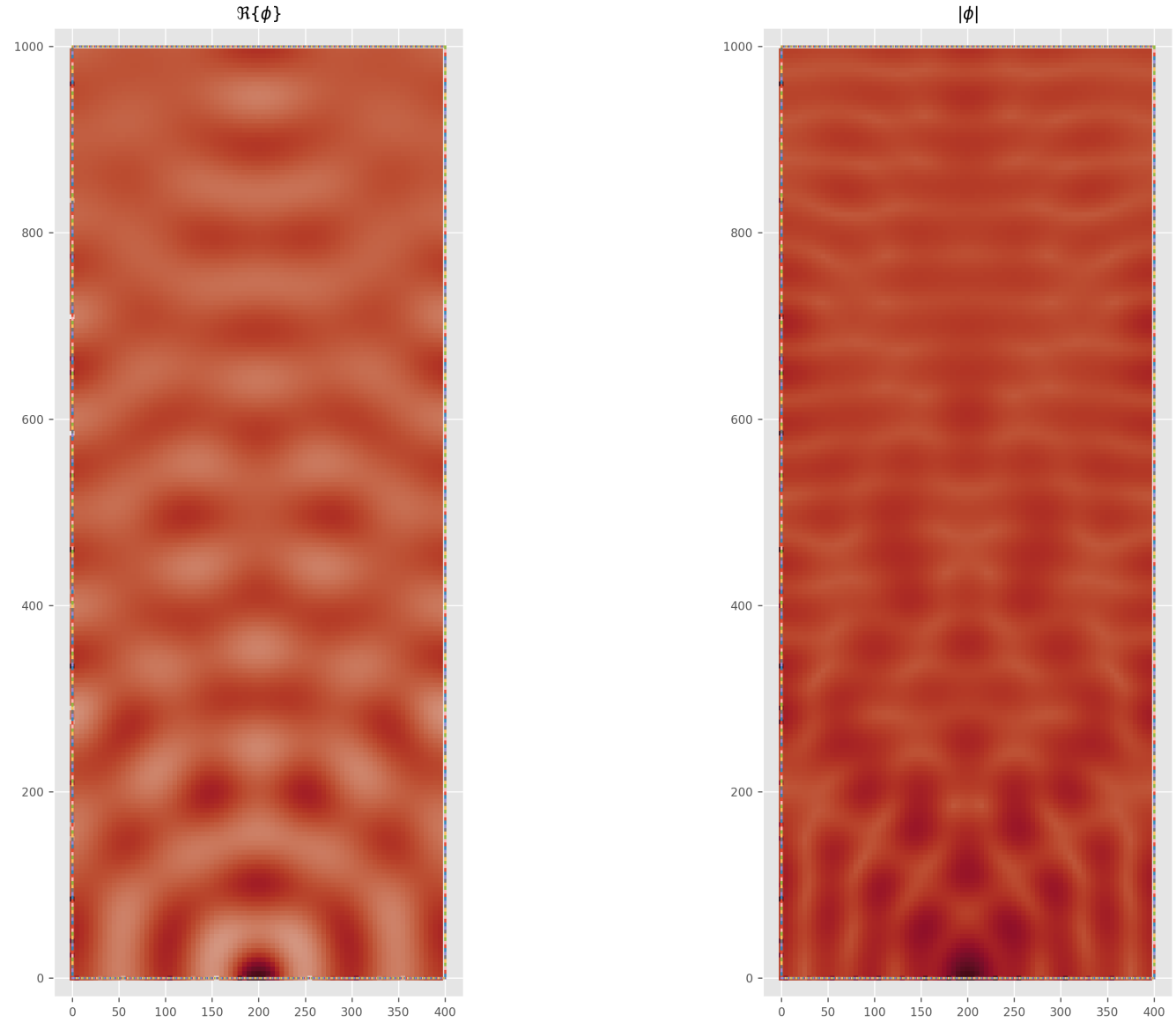

Figure 7. Breakwater (single slit) with partial reflection in the interior ($R = 0.7$ in Eq. (22)).

4.3 Breakwaters

In Figure 8 the example in Berkhoff (1976) (Fig. 3.17 therein) is attempted to be reproduced. The exact details of the setup are not given, so the case is attempted to be reconstructed as best as possible. An obliquely incident wave ($T = 3$ s) enters the harbor at the top right, and is reflected along the interior of the harbor. A reflection coefficient of 0.5 is set along the harbor, except at the two rectangular structures extending into the harbor, which are fully reflective (See Listing 4).

https://doi.org/10.5194/egusphere-2026-1198
Preprint. Discussion started: 4 May 2026

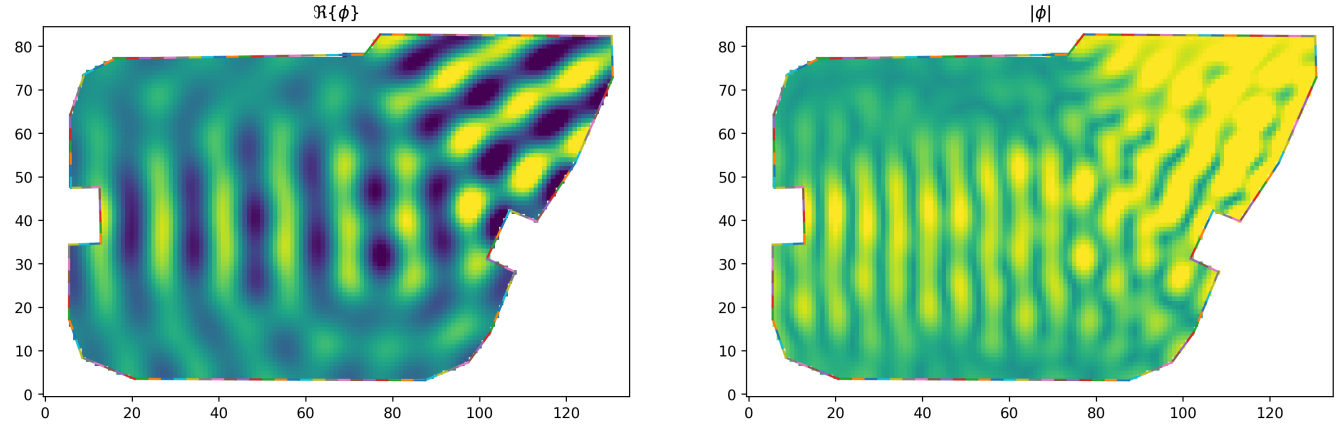

Figure 8. Breakwater as in Berkhoff (1976) (Fig. 3.17 therein) with partial reflection in the interior ($R = 0.5$), and fully reflective structures extending into the harbor. The wave field is incident obliquely from top left, entering the harbor through the opening at the top right.

Listing 4. Excerpts of code for simulating a harbor with varying reflectiveness of the harbor walls.

```
import ohbemn as oh
import pandas as pd
import numpy as np
from shapely import Polygon, Point

# Construct polygon from CSV file of XY points.
points = pd.read_csv('./fig317.csv', names=['x', 'y'])
polygon = Polygon(points.itertuples(index=False, name=None))

# Scale (optional)
# polygon = shapely.affinity.scale(polygon, 100., 100.)

# Increase resolution
polygon = polygon.segmentize(3.)

# Set up region
v, e = oh.region_from_polygon(polygon)
region = oh.Region(v, e)

T = 3.
f = 1. / T
w = 2 * np.pi * f
c, cg, k = oh.wave.wavec_interm(T=T, h=40.)
kx = -k / 2  # 45 deg. oblique direction.
ky = -np.sqrt(k**2 - kx**2)

## Reflection coefficient
R = .5
```

https://doi.org/10.5194/egusphere-2026-1198
Preprint. Discussion started: 4 May 2026

EGUsphere
Preprint repository

```
alpha = oh.rcoeff.berkoff_partial_reflection(R)
print(f"{R=} -> {alpha=}")

# define BC
normals = region.normals()
centers = region.centers()

y0 = 82.1  # opening is above this

bc = region.neumann_boundary_condition()
bi = region.boundary_incidence()

for i in range(region.len()):
    x = centers[i, :]

    if x[1] > y0:
        # Opening
        bc.alpha[i] = 1.
        bc.beta[i] = 0.
        bc.f[i] = oh.source.plane(kx, ky, *x)[0]
    else:
        if (i >= 36 and i <= 46) or (i >= 98 and i <= 108):
            # Fully refletive structures
            bc.alpha[i] = 0.
            bc.beta[i] = 1.
            bc.f[i] = 0
        else:
            # Partially reflecting boundary
            bc.f[i] = 0.
            bc.alpha[i] = alpha * k
            bc.beta[i] = 1.

# Solve the boundary
solver = oh.Solver(region)
bs = solver.solve_boundary(oh.Interior, k, c, bc, bi)

# Sample points in the interior
x = np.arange(0, 135, 1)
y = np.arange(0, 85, 1)
xx, yy = np.meshgrid(x, y)
ep = np.vstack((xx.ravel(), yy.ravel())).T

# Mask against polygon to throw out exterior points.
p = Polygon((xi[0], xi[1]) for xi in region.vertices())
ii = np.array([p.contains(Point(xi[0], xi[1])) for xi in ep])
ep = ep[ii]

# Solve interior sample points
eF = bs.solve_samples(np.zeros(ep.shape[0]), ep)

# Plot
eFp = np.full(xx.shape, np.nan, dtype=np.complex128)
```

https://doi.org/10.5194/egusphere-2026-1198
Preprint. Discussion started: 4 May 2026

```
eF = eF.phis
eFp[ii.reshape(xx.shape)] = eF

fig, ax = plt.subplots()
region.plot(ax)
ax.set_aspect('equal')
ax.pcolor(xx, yy, np.real(eFp), vmin=-1, vmax=1)
```

4.4 East-Alexandria port

The East-Alexandria port is one of the oldest in the world, with the first constructions built in the 1900 BC. Figure 9 (top) shows satellite imagery of the harbor. The double gap type harbor allows significant amounts of waves to enter, and in 62 AD 200 moored ships were reported to sink in a severe storm (Noli and Franco, 2008). Indicating that this design is not ideal. The bottom panel in Fig. 9 shows the simulated wave field for 8 second period waves arriving from the north. The interior of the harbor is set to a low reflectivity of $R = 0.1$. The shadow zone on the left (western) part, is clearly utilized by the ships visible in the satellite image. The setup of the model is very similar to the example above, shown in Listing 4.

https://doi.org/10.5194/egusphere-2026-1198
Preprint. Discussion started: 4 May 2026

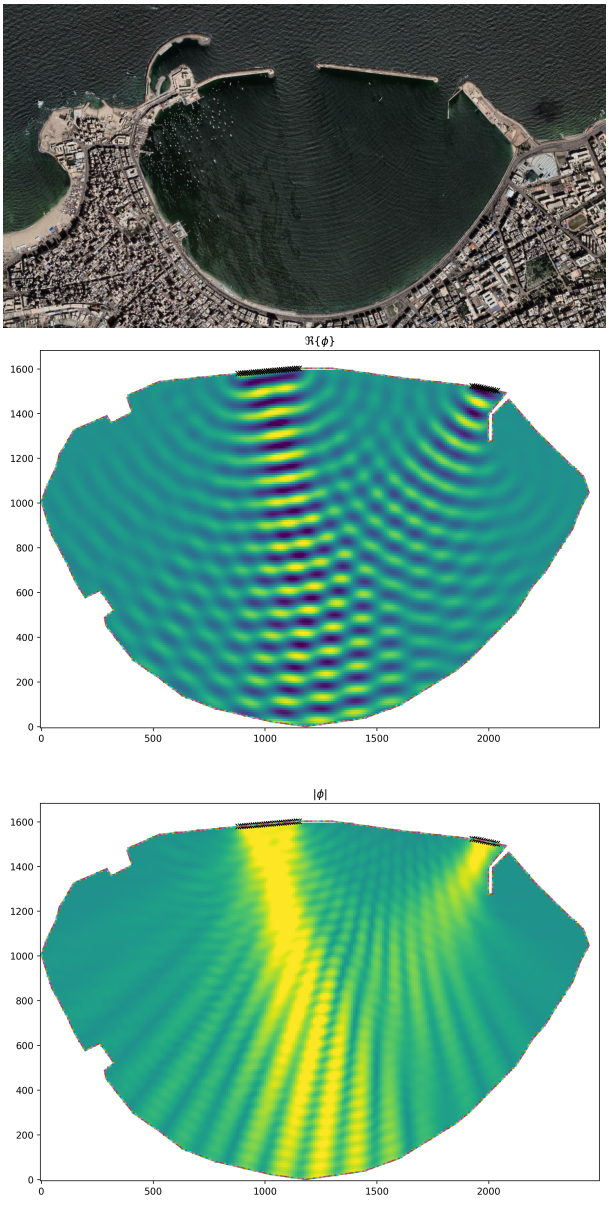

Figure 9. Top: The East-Alexandria port in in Egypt, one of the oldest ports in the world (first facilities built in 1900 BC). The width across the harbor is approximately 2450 meters. Two openings allow ships, and waves, to enter. Map data and Imagery © 2026 Google, Maxar Technologies, CNES / Airbus. **Middle:** The amplitude including phase of the modeled wave field, $\Re\{\varphi\}$. **Bottom:** The absolute amplitude of the modeled wave field, $|\varphi|$.

https://doi.org/10.5194/egusphere-2026-1198
Preprint. Discussion started: 4 May 2026

4.5 Submarine trench

A submarine trench or canyon gives an abrupt change in depth. As the wave propagates above the shallow part and encounters the edge of the trench the phase speed increases, Eq. (29). While this BEM model can compute reflection and transmission from the boundary, or total internal reflection, in order to maintain the along-boundary wave number (continuous surface, or Snell's law), it cannot handle partial reflections directly. In this case the reflection can be approximated by coupling the BEM model with other models estimating the reflection and phase change at the boundary. In Figure 10 the scattered field from the Nazaré submarine canyon (Tyler et al., 2009) is shown.

Here the incident and scattered wave field (amplitude and phase) is computed in for a dense cloud of sample points in the region of interest (outside the canyon). The wave field is computed for a plane-wave source arriving from all directions and periods for which The European Centre for Medium-Range Weather Forecasts (ECMWF) publishes their wave forecasts. At the boundary, the reflection coefficient is computed using Kirby and Dalrymple (1983)'s plane-wave approximation. At each segment of the boundary, φ_i is assigned the product of the source wave field (φ_s) and the reflection coefficient:

$$\varphi_i = -a_{r,i}\varphi_s(\mathbf{x}_i) \tag{38}$$

See Listing 5 for an excerpt of how this is implemented in the model. For each direction and period, the incident and reflected field is summed coherently. The resulting transfer function ($P_\mathbf{r}$) can be used to compute a (incoherent) response spectrum (Holthuijsen, 2007, Eq. (3.6.6) therein):

$$S_\mathbf{r}(f,\theta) = |P_\mathbf{r}(f,\theta)|^2 \tag{39}$$

The response spectrum is computed once, and may now be multiplied element-wise with a forecast or measured spectrum to model the spectrum close to shore. The integral of resulting spectrum is the variance, proportional to the significant wave height, which is shown in Figure 10.

https://doi.org/10.5194/egusphere-2026-1198
Preprint. Discussion started: 4 May 2026

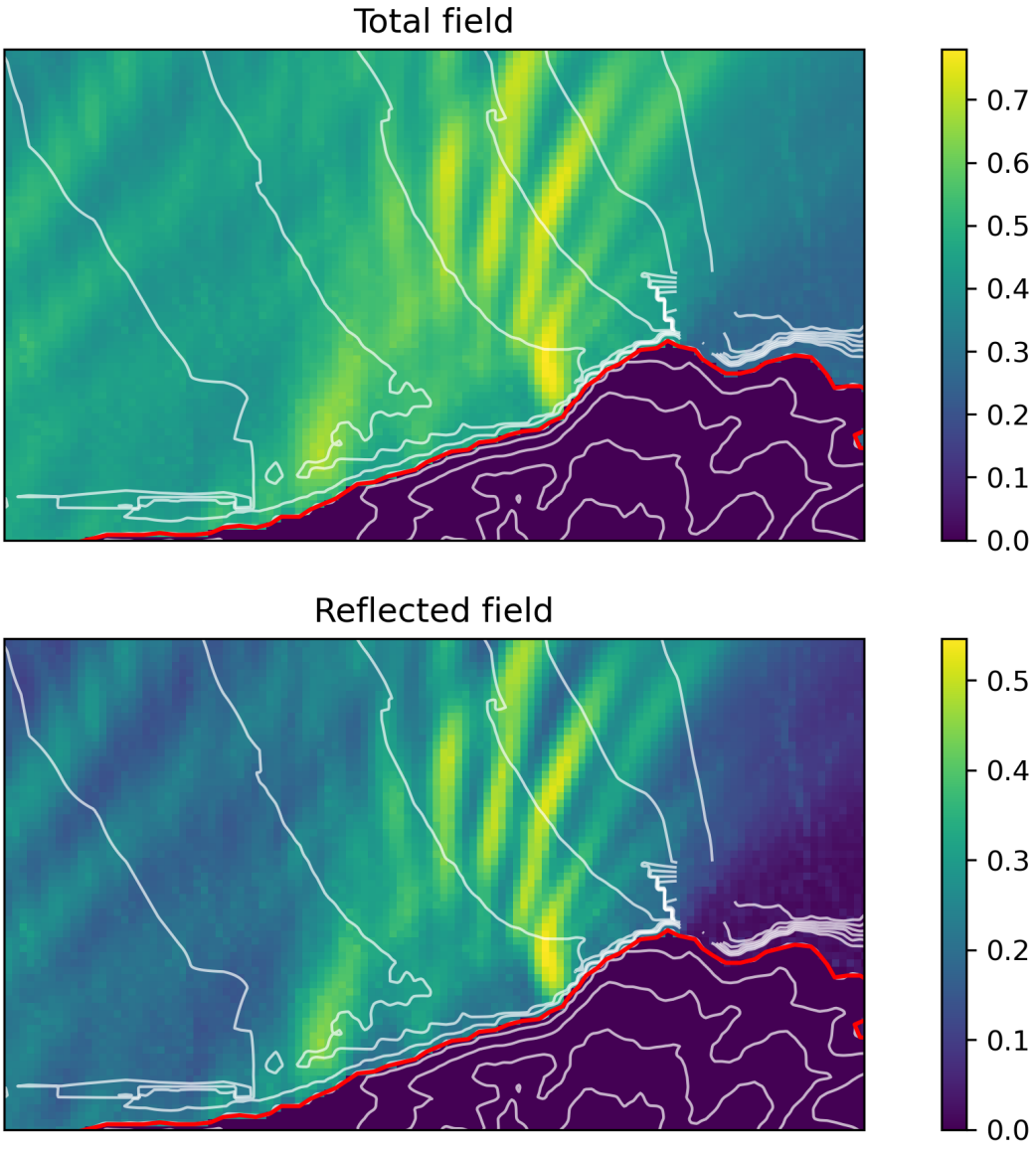

Figure 10. The variance of a scattered field from a submarine trench computed for an offshore 2D spectrum from the operational ECMWF wave forecast. Note that the colour scale is not the same in the two plots, with the lower panel representing the reflected wave field having a lower amplitude than the total field shown in the upper panel.

Listing 5. Excerpt of code for calculating reflection coefficient and assigning boundary conditions along a canyon rim for a particular wavenumber-component.

https://doi.org/10.5194/egusphere-2026-1198
Preprint. Discussion started: 4 May 2026

```
import ohbemn as oh

d1 = 20.   # shelf depth [m]
d2 = 150.  # trench depth [m]
L   = 250. # trench width [m]

# Direction and period
T = 11. # [s]
dfrom = np.deg2rad(270.) # direction from
dto = oh.rcoeff.flipdir_rad(dfrom)  # direction to
f = 1. / T # [Hz]
akx, aky, _dto = oh.rcoeff.dir_to_k_incidence(np.rad2deg(dto))
c1, cg1, k1 = oh.wave.wavec_interm(T, d1)  # above shelf
c2, cg2, k2 = oh.wave.wavec_interm(T, d2)  # above canyon
kx = akx * k1
ky = aky * k1

# Region generated from 50 m contour
region = oh.Region(vertices, edges)
bc = region.boundary_condition()

centers = region.centers()
normals = region.normals()
for i in range(region.len()):
    x = centers[i, :]
    n = normals[i, :]

    # Source
    phi = oh.source.plane(kx, ky, *x)[0]
    v = oh.source.dplane(kx, ky, *x, -n)[0]

    bc.alpha[i] = 1.
    bc.beta[i] = 0.
    bc.f[i] = 0.

    # If top of region.
    if x[1] > y1 and x[0] > x0 and x[0] < x1:
        ## Calculate reflection coefficient.

        # Incidence angle relative to normal of segment
        ai, outside = oh.rcoeff.dir_from_to_incidence(dfrom, n)
        Kr2, Kt2 = oh.rcoeff.kirby_pwa_coeff(ai, d1, d2,
                                             d1, L, 1. / T)

        # The reflected wave has approximately a 180 deg
        # phase-change. Using a complex reflection
        # coefficient would be even better.
        a_r = np.sqrt(Kr2)

        bc.f[i] = -a_r * phi
```

https://doi.org/10.5194/egusphere-2026-1198
Preprint. Discussion started: 4 May 2026

5 Conclusions

A Boundary Element Method model is implemented in *Python* and *Rust* with parallel computation of boundary coefficients and the wave field at sample points. The model is based on the BEM model for acoustic waves described by Kirkup (1998). It is adapted to ocean waves and comes with a framework for calculating source parameters and directions, constructing a boundary from a polygons, calculating sea surface elevation, and calculating reflection coefficients at trenches or partially reflecting boundaries.

The difficulty in BEM modeling is often to define the boundary conditions. These were summarized for several common cases, and in the case of a single opening breakwater, compared to a theoretical model for diffracted waves.

BEM-type models do not support wave growth, nonlinear interactions between the wave components, wave breaking (except parameterized as attenuation through a complex wave number). The wave speed, and therefore the water depth, must be constant within each domain. However, the model allows for fast computations of the wave field encountering complex domains (although in this implementation only simply-connected domains). As such, it is useful for rapid assessment of the wave conditions inside harbors and along the coast, where water depth can be assumed relatively constant (or in the case of submarine trenches, abruptly changing). As a planning tool, it offers a quick first glimpse of the salient conditions in harbors and for marine structures. More sophisticated phase-resolving models are needed for the more detailed planning (see, e.g., the fully nonlinear potential flow solver REEF::3D by Bihs et al. 2020), but for first-order assessments of the wave conditions, the boundary element method offers a fast and cheap alternative. In fact, the Norwegian Standard (NS 9415) requires to include diffraction and reflection in numerical studies of the wave field. Often these effects may not play a relevant role and are hence not worth the costs of a detailed modelling study. These are cases where this necessity could be assessed quickly and cheaply with ohbemn.

Code availability. The current version of model name is available from the project website https://github.com/gauteh/ohbemn under the *GNU General Public License v3.0 or later* licence. The exact version of the model used to produce the results used in this paper is archived on repository under DOI 10.5281/zenodo.18864058 (Hope, 2026) (version 0.2.0), as are input data and scripts to run the model and produce the plots for all the simulations presented in this paper.

Author contributions. G. Hope: Implementation, theory, manuscript. P. Bohlinger: Review of manuscript and theory. T. Halsne: Review of manuscript and theory. Ø. Breivik: Review of manuscript and theory.

Competing interests. The authors declare no competing interests.

Acknowledgements. The authors gratefully acknowledge funding by the NFR project *B-Waves* (grant 344357).

https://doi.org/10.5194/egusphere-2026-1198
Preprint. Discussion started: 4 May 2026

References

OpenFAST/Openfast, https://github.com/OpenFAST/openfast, 2025.

Ardhuin, F., Chapron, B., and Collard, F.: Observation of Swell Dissipation across Oceans, Geophysical Research Letters, 36, 2008GL037 030, https://doi.org/10.1029/2008GL037030, 2009.

Belibassakis, K., Magkouris, A., and Rusu, E.: A BEM for the Hydrodynamic Analysis of Oscillating Water Column Systems in Variable Bathymetry, Energies, 13, 3403, https://doi.org/10.3390/en13133403, 2020.

Berkhoff, J. C. W.: Mathematical Models for Simple Harmonic Linear Water Waves: Wave Diffraction and Refraction, Ph.D. thesis, TU Delft, 1976.

Bihs, H., Wang, W., Pakozdi, C., and Kamath, A.: REEF3D::FNPF—A Flexible Fully Nonlinear Potential Flow Solver, Journal of Offshore Mechanics and Arctic Engineering, 142, 041 902, https://doi.org/10.1115/1.4045915, 2020.

Chakrabarti, A. and Sahoo, T.: On the Incoming Water Waves against a Vertical Cliff, Proceedings of the Indian Academy of Sciences - Section A, 107, 89–93, https://doi.org/10.1007/BF02840476, 1997.

Collard, F., Ardhuin, F., and Chapron, B.: Monitoring and Analysis of Ocean Swell Fields from Space: New Methods for Routine Observations, Journal of Geophysical Research: Oceans, 114, 2008JC005 215, https://doi.org/10.1029/2008JC005215, 2009.

Hall, M., Housner, S., Zalkind, D., Bortolotti, P., Ogden, D., and Barter, G.: An Open-Source Frequency-Domain Model for Floating Wind Turbine Design Optimization, Journal of Physics: Conference Series, 2265, 042 020, https://doi.org/10.1088/1742-6596/2265/4/042020, 2022.

Halsne, T., Christensen, K. H., Hope, G., and Breivik, Ø.: Ocean Wave Tracing v.1: A Numerical Solver of the Wave Ray Equations for Ocean Waves on Variable Currents at Arbitrary Depths, Geoscientific Model Development, 16, 6515–6530, https://doi.org/10.5194/gmd-16-6515-2023, 2023.

Hecht, F.: FreeFEM Documentation v4.13, Tech. rep., 2026.

Holthuijsen, L. H.: Waves in Oceanic and Coastal Waters, Cambridge University Press, 2007.

Hope, G.: Oh Bemn! Ocean Surface Wave Boundary Element Method, Zenodo, https://doi.org/10.5281/zenodo.18864058, 2026.

Irving, B., Castelao, G. P., Beyers, C., Clemson, J., Krieger, J., Marechal, G., Pizzo, N., and Bôas, B. V.: Mantaray: A Rust Package for Ray Tracing Ocean Surface Gravity Waves, Journal of Open Source Software, 10, 8691, https://doi.org/10.21105/joss.08691, 2025.

Isaacson, M. and Qu, S.: Waves in a Harbour with Partially Reflecting Boundaries, Coastal Engineering, 14, 193–214, https://doi.org/10.1016/0378-3839(90)90024-Q, 1990.

Jargstorff, F.: Fjargsto/Abem, https://github.com/fjargsto/abem, 2025.

Jensen, F. B., Kuperman, W. A., Porter, M. B., and Schmidt, H.: Computational Ocean Acoustics, Springer New York, New York, NY, ISBN 978-1-4419-8677-1 978-1-4419-8678-8, https://doi.org/10.1007/978-1-4419-8678-8, 2011.

Jiang, H., Stopa, J. E., Wang, H., Husson, R., Mouche, A., Chapron, B., and Chen, G.: Tracking the Attenuation and Nonbreaking Dissipation of Swells Using Altimeters, Journal of Geophysical Research: Oceans, 121, 1446–1458, https://doi.org/10.1002/2015JC011536, 2016.

Kinsman, B.: Wind Waves, 1965.

Kirby, J. T. and Dalrymple, R. A.: Propagation of Obliquely Incident Water Waves over a Trench, Journal of Fluid Mechanics, 133, 47–63, https://doi.org/10.1017/S0022112083001780, 1983.

Kirkup, S.: The Boundary Element Method in Acoustics: A Development in Fortran, no. 1 in Integral Equation Methods in Engineering, Integrated Sound Software, Hebden Bridge, ISBN 978-0-9534031-0-3, 1998.

https://doi.org/10.5194/egusphere-2026-1198
Preprint. Discussion started: 4 May 2026

Kirkup, S.: The Boundary Element Method in Acoustics: A Survey, Applied Sciences, 9, 1642, https://doi.org/10.3390/app9081642, 2019.

Kirkup, S. M.: Solution of Discontinuous Interior Helmholtz Problems by the Boundary and Shell Element Method, Computer methods in applied mechanics and englneerlnging, 1997.

Kurnia, R. and Ducrozet, G.: NEMOH: Open-source Boundary Element Solver for Computation of First- and Second-Order Hydrodynamic Loads in the Frequency Domain, Computer Physics Communications, 292, 108 885, https://doi.org/10.1016/j.cpc.2023.108885, 2023.

Lamb, H.: Hydrodynamics, 6th edn., 1932.

Li, Y., Zheng, Y., Lin, Z., Adcock, T. A. A., and van den Bremer, T. S.: Surface Wavepackets Subject to an Abrupt Depth Change. Part 1. Second-order Theory, Journal of Fluid Mechanics, 915, A71, https://doi.org/10.1017/jfm.2021.48, 2021.

Liu, Y.: Introduction of the Open-Source Boundary Element Method Solver HAMS to the Ocean Renewable Energy Community.

Noli, A. and Franco, L.: The Ancient Ports of Rome: New Insights from Engineers, Tech. rep., 2008.

Penney, W. G. and Price, A. T.: Part I. The Diffraction Theory of Sea Waves and the Shelter Afforded by Breakwaters, Philosophical Transactions of the Royal Society of London. Series A, Mathematical and Physical Sciences, 244, 236–253, https://doi.org/10.1098/rsta.1952.0003, 1952.

Pos, J. D. and Kilner, F. A.: Breakwater Gap Wave Diffraction: An Experimental and Numerical Study, Journal of Waterway, Port, Coastal, and Ocean Engineering, 113, 1–21, https://doi.org/10.1061/(ASCE)0733-950X(1987)113:1(1), 1987.

Raghavan, V., Lavidas, G., and Metrikine, A. V.: Comparing Open-Source BEM Solvers for Analysing Wave Energy Converters, Journal of Physics: Conference Series, 2647, 072 002, https://doi.org/10.1088/1742-6596/2647/7/072002, 2024.

Raichlen, F. and Lee, J.-J.: AN INCLINED-PLATE WAVE GENERATOR, Coastal Engineering, 1978.

Sanchez-Brea, L. M., Soria-Garcia, A., Andres-Porras, J., Pastor-Villarrubia, V., Elshorbagy, M. H., Muñoz, J. d. H., Torcal-Milla, F. J., and Alda, J.: Diffractio: An Open-Source Library for Diffraction and Interference Calculations, in: Optics and Photonics for Advanced Dimensional Metrology III, vol. 12997, pp. 236–243, SPIE, https://doi.org/10.1117/12.3021879, 2024.

Sgallari, F.: A Boundary Integral Equation Approach to Wave Propagation over a Trench, Applied Mathematical Modelling, 7, 33–40, https://doi.org/10.1016/0307-904X(83)90160-9, 1983.

Shen, F. and Wang, A.: Fast-Fourier-transform Based Numerical Integration Method for the Rayleigh-Sommerfeld Diffraction Formula, Applied Optics, 45, 1102–1110, https://doi.org/10.1364/AO.45.001102, 2006.

Sommerfeld, A.: Die Greenische Funktionen Der Schwingungsgleichung, in: Jahresbericht Der Deutschen Mathematiker-Vereinigung, p. 309, 1912.

Tyler, P., Amaro, T., Arzola, R., Cunha, M. R., Stigter, H. D., Gooday, A., Huvenne, V., Ingels, J., Kiriakoulakis, K., Lastras, G., Masson, D., Oliveira, A., Pattenden, A., Vanreusel, A., Weering, T. V., Vitorino, J., Witte, U., and Wolff, G.: Europe's Grand Canyon Nazaré Submarine Canyon, Oceanography, 22, 46–57, 2009.

Viswanathan, S., Holden, C., Egeland, O., and Greco, M.: An Open-Source Python-Based Boundary-Element Method Code for the Three-Dimensional, Zero-Froude, Infinite-Depth, Water-Wave Diffraction-Radiation Problem, Modeling, Identification and Control: A Norwegian Research Bulletin, 42, 47–81, https://doi.org/10.4173/mic.2021.2.2, 2021.

Zabala, I., Peña-Sanchez, Y., Kelly, T., Henriques, J., Penalba, M., Faedo, N., Ringwood, J., and Blanco, J. M.: BEMRosetta: An Open-Source Hydrodynamic Coefficients Converter and Viewer Integrated with Nemoh and FOAMM, in: 14th European Wave and Tidal Energy Conference, Plymouth, UK, 2021.